J Solid State Electrochem (2006) 10: 48–53
DOI 10.1007/s10008-005-0660-z

ORIGINAL PAPER

KunWei Li · XiaoTian Meng
Xue Liang · Hao Wang · Hui Yan

Electrodeposition and characterization of PbSe films on indium tin oxide glass substrates

Received: 6 December 2004 / Revised: 10 January 2005 / Accepted: 3 February 2005 / Published online: 9 March 2005

Abstract Electrodeposition of lead selenide (PbSe) thin films on indium tin oxide (ITO) covered glass is described. While disodium salt of ethylenediaminetetraaceticacid was used to complex the lead ions, well crystallized, nearly stoichiometric and mirror-like PbSe films were deposited on ITO glass in potentiostatic mode using aqueous acidic electrolyte containing Pb and Se precursors at different bath temperature. The improvement of crystallinity of the PbSe films deposited at different temperature was studied using X-ray diffraction and Raman scattering. The morphology and composition of the films were characterized by scanning electron microscopy and energy disperse analysis by X-ray, respectively. The optical property of the film was studied by optical measurement techniques.

Keywords PbSe · Electrodeposition · Raman scattering

Introduction

Thin solid films of metal chalcogenide have been a subject of interest for many years mainly because of their possible application to the manufacture of large-area photodiode arrays, solar selective coatings, solar cells, photoconductors, sensors etc. Among these metallic chalcogenide, lead selenide (PbSe) is an interesting narrow band-gap IV–VI compound semiconductor (Eg = 0.26 eV), which is used in photodetectors, photoresistors and photoemitters in the infrared (IR).

Lead selenide has been synthesized by various methods, including chemical bath deposition [1], vacuum deposition [2], sputtering, spray pyrolysis, electrodeposition [3], sonochemistry [4] and sonoelectrochemistry [5], and microwave heating [6]. Electrodeposition has been used to prepare high-quality metal selenide thin films, with advantages such as low-temperature deposition and relatively low-cost hardware [7]. Streltsov et al. [8] and Molin et al. [3] studied the mechanism of PbSe electrodeposition from aqueous solutions on platinum plates and titanium plates, respectively. Saloniemi et al. [9, 10] have extensively studied the electrodeposition of PbSe films, and various influential parameters such as substrates, electrodeposited potential and the electrolyte components were investigated. However, in their papers, most of the studies were mainly focused on the electrodeposition mechanism.

As a transparent electrode, indium tin oxide (ITO) is a well-known semiconductor, which has many advantages such as low price, high conductivity and higher transparency. The optical transmittance of ITO equals to 75∼85% in the range between 360 nm and 2,500 nm. If the non-transparent materials such as platinum or titanium were used as the electrodes, it would inevitably absorb incident photons and degrade the responsivity of optoelectronic devices. Therefore, as a potential candidate for infrared detector and photoconductor, the synthesis and characterization of PbSe films electrodeposited on ITO-covered glass need more researches.

This paper reports the electrodeposition and characterization of PbSe films formed on ITO-covered glass. The effects of deposition time and temperature on the compositions and phases of films were investigated. The as-deposited films were characterized using X-ray diffraction (XRD), Raman spectroscopy and transmission spectrum.

Experimental

The plating experiments were carried out from the solutions containing analytical grade lead acetate [$Pb(CH_3COO)_2$], selenium dioxide (SeO_2) and a disodi-

K. Li · X. Meng · X. Liang
H. Wang (✉) · H. Yan
The College of Materials Science and Engineering,
Beijing University of Technology,
Beijing, 100022, China
E-mail: haowang@bjut.edu.cn
Tel.: +86-10-67392733
Fax: +86-10-67392412

um salt of ethylenediaminetetraaceticacid (Na_2-EDTA) in deionized water. The chemicals were used as received. In all experiments, the concentration of lead(II) acetate was kept at 0.01 M, Na_2-EDTA 0.1 M and selenium dioxide 0.001 M. The pH of the electrolyte was maintained at 4. The Na_2-EDTA was used to complex the lead ions. All experiments were performed under unstirred condition in potentiostatic mode unless otherwise stated.

A conventional three-electrode cell was used with the platinum foil (3×3 cm) as a counter electrode, ITO-covered glass plates (1×4 cm size) as a working electrode and a saturated calomel electrode (SCE) as the reference electrode. One square centimeter area of working electrode was exposed to the electrolyte and the rest area was covered with an insulating tape. The distance between anode and cathode was kept fixed at 0.4 cm throughout the experiments. The reference electrode made contact with the electrolyte bath via a salt bridge. The working electrode potential was monitored by a potentiostat. All potentials quoted are versus SCE except otherwise stated.

The thickness of the as-prepared films was measured by a Surfcom 480 A (Tokyo Seimitsu) profilometer. The structural characterization of the films was carried out by using a Bruker Advance D8 X-ray diffractometer equipped with Gobel Mirror and Cu Kα radiation ($\lambda = 1.5406$ Å) and a total pattern analysis system (TOPAS) program. The mode of grazing incidence diffraction (GID), the step time of 1 s and scanning rate of 0.02°/s were used to record the pattern in the range of 20°~70°. A Hitachi scanning electron microscope, S-3500N, equipped with X-ray energy dispersion analysis, OXFORD F-2300X, was employed to study the morphology and the chemical composition of the electrodeposited films. Raman spectra of the films were recorded on a JY-T64000 (Jobin-Yvon) Raman spectrometer equipped with a solid laser of Coherent Verdi-2. Optical transmission was performed in the wavelength range 200~2,500 nm using a UV-VIS-NIR spectrophotometer (Shimadzu UV-3101PC).

Results and discussion

In order to find the suitable potential range for the deposition of PbSe, the polarization curves for the reduction of electrolyte were recorded at potentiostatic mode. Figure 1 shows the polarization curves for the bath containing electrolyte (containing 0.01 M $Pb(CH_3COO)_2$, 0.1 M Na_2-EDTA and 0.001 M SeO_2) at pH 4 and the temperature of 20 °C, onto ITO-covered glass substrate. The curve in Fig. 1 has three zones: the first between −0.6 and −0.8 V, the second between −0.80 and −1.05 V, and the third at more negative potentials than 1.05 V. The first zone mainly ascribed to the deposition of selenium. The formation of elemental selenium was evidenced by holding the

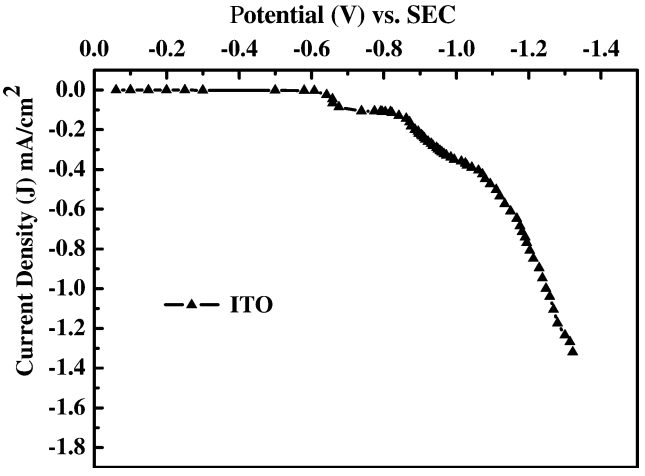

Fig. 1 Polarization curves for the reduction of electrolyte (containing 0.01 M $Pb(CH_3COO)_2$, 0.1 M Na_2-EDTA and 0.001 M SeO_2) onto ITO-covered glass at pH 4 and the temperature of 20 °C

substrate at a constant potential of −0.7 V vs. SCE and observing the appearance of a reddish selenium deposit. When the constant potential equals to −0.9 V, evident silvery films were gained, which contain more lead. The third zone mainly may be ascribed to the formation of hydrogen, a lot of bubbles formed on cathode while the deposition potential equals to −1.15 V. The PbSe deposition potential was chosen as −0.8 V for ITO-covered glass, which is consistent with the thermodynamic analysis of Kröger [11] that PbSe can be electrodeposited at a deposition potential between potentials of their constituents. The results of energy disperse analysis by X-ray (EDAX) listed in Table 1 also support this choice.

Table 1 shows the compositions and main phases of the films electrodeposited under different conditions. The results show that different deposition potential affected the compositions and main phases of films. At the potential of −0.7 V, the reddish selenium films were gained while silvery lead films gained at −0.9 V. PbSe films can be obtained at −0.8 V and nearly stoichiometric films were got at 50 °C for 10 min. In general, the PbSe films prepared by electrodeposition are selenium-rich [8], and these phenomena were also observed in other selenides such as ZnSe [12], CdSe [13, 14] and EuSe [15].

Figure 2 shows the dependence of the thickness of PbSe films on the deposition time at 20 °C. The film thickness increases rapidly in the initial stage, then reaches a maximum and declines for the further deposition time. This phenomenon can be explained by considering the two competing processes taking place in the solution: one process includes the deposition of PbSe, which leads to the film growth; the other one involves the reaction of PbSe with acid in the solution, which results in the decrease of film thickness. In the initial stage of the electrodeposition, the source materials are sufficient and the solution has a high conductivity, the process of deposition plays a more important

Table 1 Composition of the films electrodeposited under different conditions

Potential of electrodeposition, E (V)	Temperature of electrodeposition, T (°C)	Time of electrodeposition, t (min)	Content of elements (atomic %)		Main phase
			Pb	Se	
−0.9	20	10	85	15	Pb (Crystalline)
−0.8	80	10	47	53	PbSe (Crystalline)
	50	10	49	51	
	20	30	44	56	
		15	43	57	
		10	45	55	
		5	16	84	Se (Amorphous)
−0.7	20	20	10	90	

role than the dissolution process, leading to the increase in film thickness. With the deposition time being prolonged, the thickness of the film increases; at the same time the resistance of film increases. So, the density of electrons decreased relatively and the PbSe film was eroded by acid in the solution. Therefore, after a certain deposition time, the dissolution process predominates over the deposition, resulting in the decrease of film thickness.

Figure 3 shows the XRD patterns of PbSe films electrodeposited for a different time at 20 °C. From Fig. 3, we can see that when the electrodeposition time is 5 min, the peaks of the profile mainly correspond with the standard data (JCPDF 88-0773) for polycrystalline ITO. However, Fig. 2 shows that the film thickness is about 50 nm when electrodeposition time is 5 min. The product could be a thin film of the amorphous selenium, which is not evidently detectable by XRD, as only a small amount of amorphous selenium is exhibited at 20°–35°. The reddish color and results of EDAX listed in Table 1 support this theory. When the electrodeposition time was 10 min, the peaks of PbSe became outstanding against those of ITO. The reflections were compared against standard JCPDS-ICDD diffraction patterns (JCPDF 06-0354). The profile was fitted to the rock salt structure PbSe with cubic cell. However, with the electrodeposition time became longer, the relative intensity of PbSe peaks against those of ITO decreased. When the electrodeposition time was further extended to 30 min, the surface of the film becomes rough. The resultant film thickness and rough surface at 30 min meant that the PbSe film may be eroded by acidic solution.

Figure 4 shows the XRD patterns of thin films electrodeposited for 10 min at 20, 50 and 80 °C. From Fig. 4 we can see that the intensities of the signal from ITO substrate decrease upon the increase of the temperature. At 80 °C, the signal from ITO almost cannot be detected since the film may be thicker than that prepared at lower temperature. The thicker film at 80 °C may have resulted because the deposition rate usually increases with deposition temperature. This hypothesis

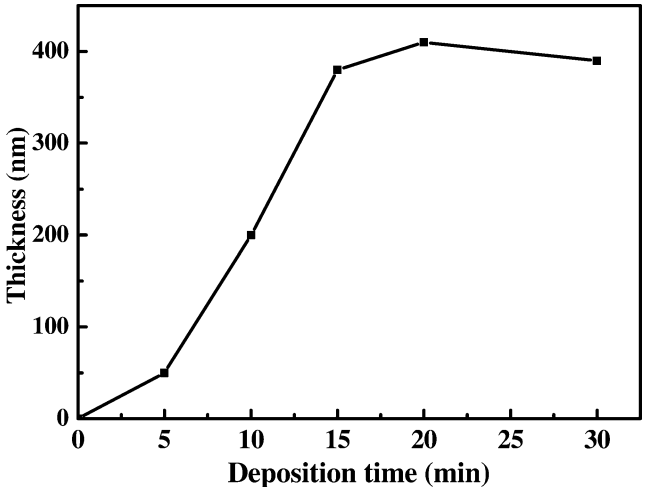

Fig. 2 The thickness of PbSe films with variation deposition time at 20 °C

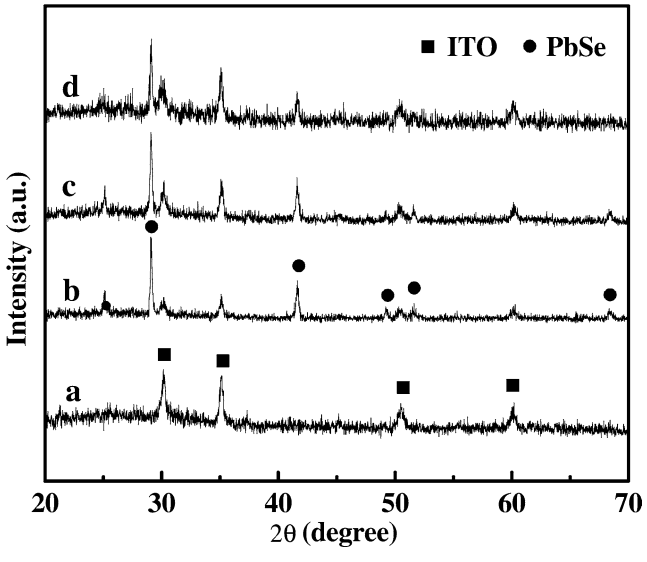

Fig. 3 X-ray diffraction (XRD) patterns of PbSe films electrodeposited at different time (**a** 5 min; **b** 10 min; **c** 15 min; **d** 30 min) at 20 °C

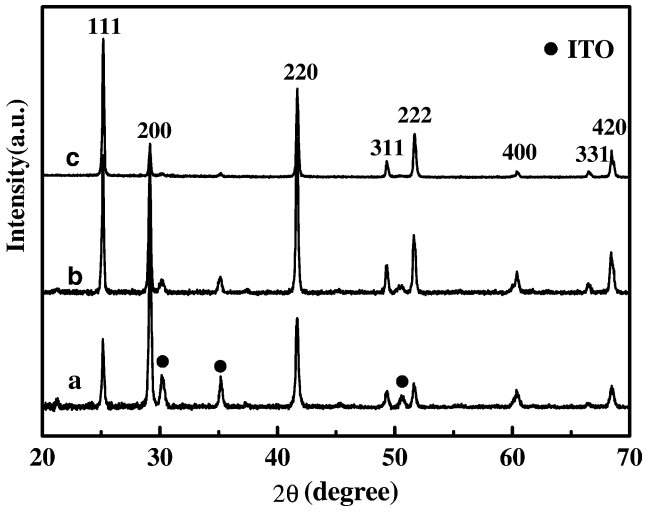

Fig. 4 X-ray diffraction pattern of PbSe films electrodeposited at different temperature (**a** 20 °C; **b** 50 °C; **c** 80 °C) for 10 min

was verified by the thickness measurement results of films which were 200, 230 and 270 nm at 20, 50 and 80 °C, respectively. Meanwhile, it is noted that different thickness induced the preferred orientation in the diffractograms. The relative intensity ratio of the peak 111 to 200 is 0.328, 0.944, and 4.07 at 20, 50 and 80 °C, respectively. The accurate FWHM values of the peaks for the samples were determined by TOPAS program, which is a graphics-based profile analysis program built around a general non-linear least squares fitting system. Being a linear combination of Cauchyian and Gaussian functions, the pV function was selected as it was the most reliable peak-shape function and was being widely used in the structure refinement software. The process of successive profile refinements modulated different structural and microstructural parameters of the simulated pattern to fit the experimental diffraction pattern. Profile refinement continues until convergence is reached in each case, with the value of the quality factor (GoF = Rwp/ Rexp) approaching close to 1. The FWHM values of the peaks for the samples obtained at different temperatures with the GoF:1.27 at 20 °C; 1.21 at 50 °C; 0.84 at 80 °C are shown in Table 2. As can be seen from Table 2 the FWHM value of each peak is less than 0.5° and with the increase of temperature the value decreases. These results suggest that the films are well crystallized and there is only a little change in crystalline degree in the three samples. However, these little differences among the crystallinity are difficult to identify with the naked eye without professional computational analysis.

The measurement of Raman spectrum of a crystal is one of the main methods to obtain information about its lattice dynamics. Raman scattering measurement was carried out at room temperature on PbSe surface by using 532 nm line from a solid laser. The excitation laser was focused on PbSe surface by a microscope and the light spot size is about 2 μm in diameter. Scattered light was collected by back-scattering configuration. No special attention was paid to polarization of the incident and scattered light.

Figure 5 shows the Raman spectra of thin films deposited at 20, 50 and 80 °C for 10 min. From Fig. 5, we can see that the dominant peak is at 139.7 cm^{-1} and the weaker peaks locate at 84.9 and 279.6 cm^{-1}. The longitudinal optical (LO) phonon is designated to the dominant peak at 139.7 cm^{-1}. It is an elementary transition. The energy of the measured LO phonon is 17.3 meV. The weaker structure at about 279 cm^{-1} is associated with two phonon scattering (2LO). The peak at about 84.9 cm^{-1} is possibly due to the longitudinal optical and the transverse optical (LO–TO) band. However, the value of the phonon energy calculated by Hall and Raceffe [16] for PbSe LO phonon at Γ point determined by inelastic tunneling at 4.2 K equals 16.5 meV. The Raman shifts measured at room temperature in this study are slightly larger than the calculated result. The blue shifts of the measured phonons may be attributed to the temperature effects because PbSe material has very low thermal conductivity. The Raman shift due to temperature effect can be qualitatively understood in terms of the anharmonic forces coupled to other vibration at the Raman phonon and thermal expansion of the lattice in the crystal [17].

It is noted in Fig. 5 that the Raman peaks of the 50 and 80 °C film are well-defined, while the dominant peak at 139.7 cm^{-1} of 20 °C film is broadened and the other two peaks are poorly recognized. The decrease of the area under the curve and the FWHM can be attributed to the improvement in the crystallinity of the films deposited at higher temperature. It indicates that the PbSe film deposited at 50 and 80 °C are well crystallized and the 20 °C film is poorly crystallized. The different results characterized by XRD (shown in Fig. 4) and Raman spectra can be explained considering the different mechanism of these two techniques. XRD patterns come from the diffraction of X-ray reflected from many

Table 2 The FWHM values of the peaks for the samples obtained at different temperatures with the GoF: 1.27 at 20 °C; 1.21 at 50 °C; 0.84 at 80 °C)

Peaks (*h*, *k*, *l*)	111	200	220	311	222	400	331	420
FWHM (degree) 20°C	0.1835025	0.1918507	0.221752	0.268188	0.275333	0.342982	0.278013	0.313758
FWHM (degree) 50°C	0.16333	0.1768676	0.194064	0.18167	0.220664	0.257623	0.275386	0.227164
FWHM (degree) 80°C	0.1386431	0.152385	0.157738	0.142197	0.174661	0.179031	0.224857	0.174009

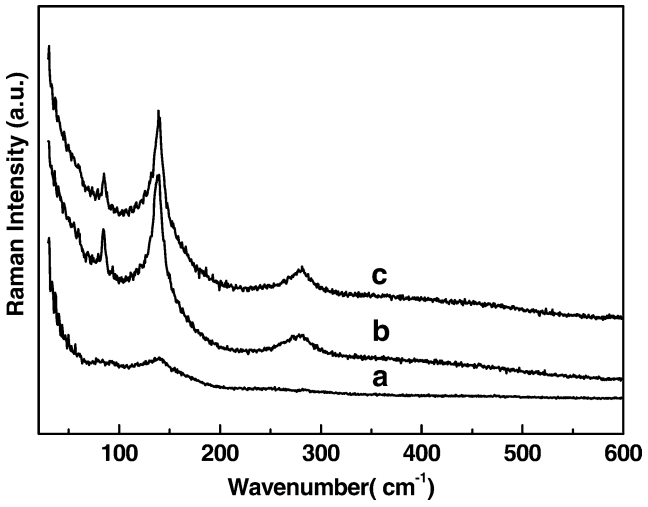

Fig. 5 Raman spectra of PbSe films deposited at different temperature (**a** 20 °C; **b** 50 °C; **c** 80 °C) for 10 min

parallel crystallographic planes, which reflect the collection of average crystallinity. Whereas, the Raman spectra come from the light scattering, it is a short-range order probe. The Raman scattering is sensitive to small disorders, even at regions as small as few unit cells [18]. Therefore, in order to get a really well-crystallized film, the higher temperature is a good choice.

Figure 6 shows the SEM images of the thin films. As can be seen from the images, the grain size of the films deposited at the temperature of 20, 50 and 80 °C was estimated to be about 180, 300 and 400 nm, respectively. With the increase of the temperature, the grain size of the thin films becomes large. The improvement of crystallinity of the PbSe films deposited at higher temperature is consistent with the results of Raman spectra. Second, it is interesting to point out the high compactness of these films.

The optical transmittance spectra of as-deposited PbSe films with the thickness of (a) 180 nm and (b) 400 nm at 20 °C are shown in Fig. 7, which is consistent with the previously reported values [19]. PbSe is known as a material of interest in the near infrared region of the electromagnetic spectrum, and therefore the optical spectra of the PbSe films were taken in the region between 200 nm and 2,500 nm, i.e., UV-VIS-NIR region. The spectrum of 180 nm films shows a gradually increasing transmittance throughout the NIR region which nearly is linear between 800 nm and 2,300 nm, whereas the spectrum of 400 nm films has an evident peak at 1,500 nm. The linear relationship between transmittance and wavelength makes it possible for this material to be used as an infrared detector.

Fig. 6 Scanning electron microscopic image of the PbSe films deposited at different temperature (**a** 20 °C; **b** 50 °C; **c** 80 °C) for 10 min

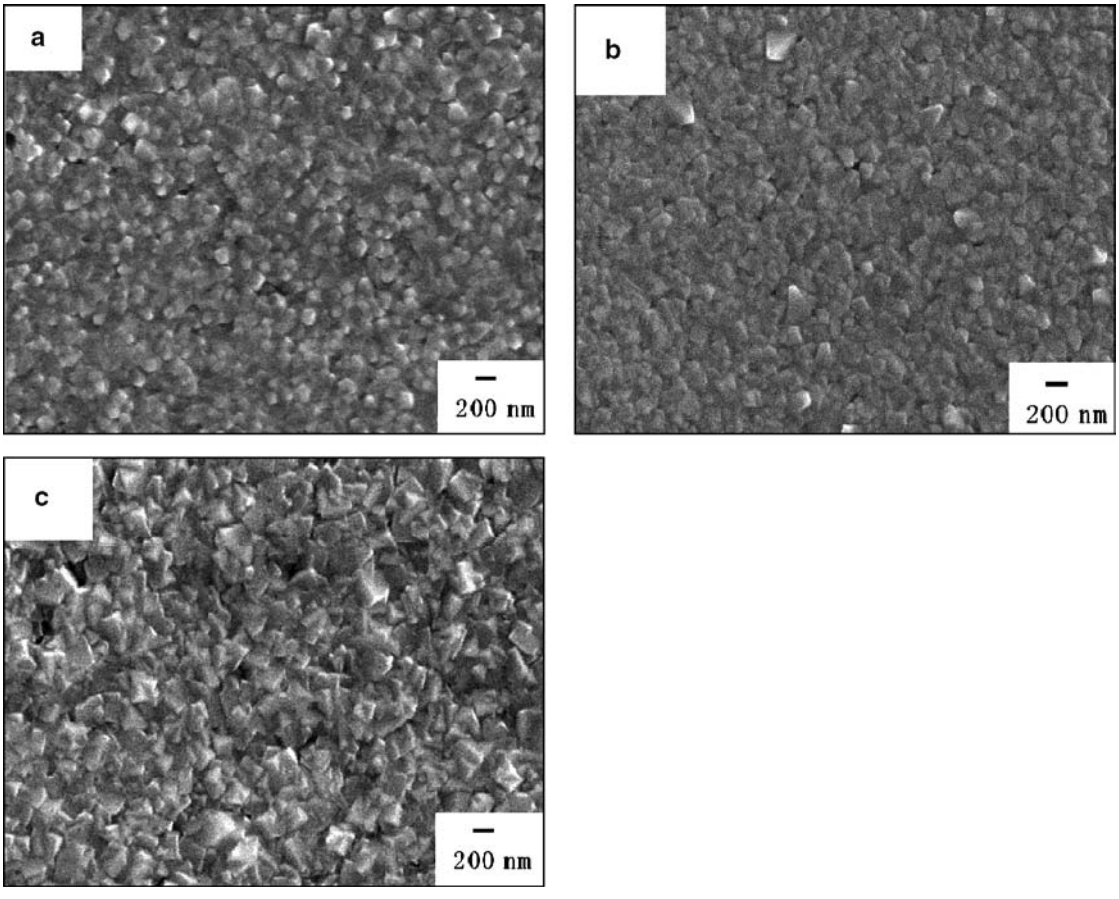

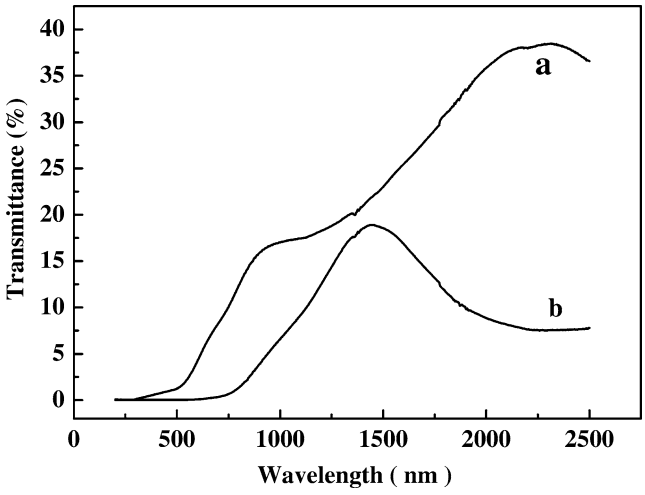

Fig. 7 The transmittance spectra of PbSe film as a function of film thickness (**a** 180 nm; **b** 400 nm)

Conclusions

In summary, high-quality PbSe films were grown on ITO-covered glass substrates by using electrochemical deposition. The suitable deposition potential was estimated from polarization curves. The relationship between the thickness of PbSe films and the deposition time was exposed. The results taken from XRD patterns are inconsistent with those of Raman spectra to some extent, which resulted from the different mechanism between the two techniques. The study of the film's optical properties shows that PbSe films are possible to be used as an infrared detector.

Acknowledgements The authors are grateful to the Project of New Star of Science & Technology of Beijing for financial support.

References

1. Schmidt G (1992) Chem Rev 92:1709
2. Das VD, Bhat KS (1990) J Mater Sci 1:169
3. Molin AN, Dikusar AI (1995) Thin Solid Films 265:3
4. Li B, Xie Y, Huang J, Qian YT (1999) Ultrason Sonochem 6:217
5. Zhu JJ, Aruna ST, Koltypin Y, Gedanken A (2000) Chem Mater 12:143
6. Zhu JJ, Palchik O, Chen SG, Gedanken A (2000) J Phys Chem 104:7344
7. Gaikwad NS, Bhosale CH (2002) Mater Chem Phys 76:198
8. Streltsov EA, Osipovich NP, Ivashkevich LS, Lyakhov AS, Sviridov VV (1998) Electrochim Acta 43:869
9. Saloniemi H, Kanniainen T, Ritala M, Leskela M, Lappalainen R (1998) J Mater Chem 8:651
10. Saloniemi H, Kemell M, Ritala M, Leskela M (2000) J Mater Chem 10:519
11. Kröger FA (1978) J Electrochem Soc 125:2028
12. Natarajan, Sharon M, Lecy-Clement C, Neumann-Spallart M (1994) Thin Solid Films 237:118
13. Skyllas Kazacos M, Miller B (1980) J Electrochem Soc 127(4):869
14. O'Bockris JM, Reddy AKN (1970) Modern electrochemistry, vol 2. Plenum, New York, p 884
15. Gaikwad S, Bhosale CH (2002) Mater Chem Phys 76:198
16. Hall RN, Racette JH (1961) J Appl Phys 32(Suppl):2078
17. Loudon R (1964) Adv Phys 13:423
18. Lanciotti F, Pizani PS, Santos IA et al (2001) J Phy Chem Solids 62:1247
19. Grozdanov I, Najdoski M, Dey SK (1999) Mater Lett 38:28